Available online at www.sciencedirect.com
ScienceDirect
Biochemical and Biophysical Research Communications 351 (2006) 240–245
BBRC
www.elsevier.com/locate/ybbrc

Effects of perfluorooctane sulfonate on action potentials and currents in cultured rat cerebellar Purkinje cells

Kouji H. Harada [a], Takahiro M. Ishii [b], Kenji Takatsuka [b], Akio Koizumi [a,*], Harunori Ohmori [b]

[a] *Department of Health and Environmental Sciences, Kyoto University Graduate School of Medicine, Kyoto 606-8501, Japan*
[b] *Department of Physiology, Faculty of Medicine, Kyoto University, Kyoto 606-8501, Japan*

Received 14 September 2006
Available online 23 October 2006

Abstract

Recently, PFOS was reported to be ubiquitously detected in the environment, as well as in human serum, raising concerns regarding its health risks. We investigated the effects of PFOS on action potentials and currents in cultured rat cerebellar Purkinje cells using whole-cell patch-clamp recording. In current-clamp experiments, PFOS significantly decreased the action potential frequency during current injection, the maximum rate of fall and the threshold of action potential, and negatively shifted the resting membrane potential at doses over 30 μM. In voltage-clamp experiments, PFOS shifted the half-activation and inactivation voltages of I_{Ca}, I_{Na}, and I_K toward hyperpolarization at 30 μM. I_{HCN1} expressed in *Xenopus* oocytes was similarly affected. Incorporation of PFOS into the cell membrane probably increased the surface negative charge density, thereby reducing the transmembrane potential gradient and resulting in hyperpolarizing shifts of both the activation and inactivation of ionic channels. These findings indicate that PFOS may exhibit neurotoxicity.

Keywords: Perfluorooctane sulfonate; Rat cerebellar Purkinje cell; Membrane surface charge

Perfluorooctane sulfonate (PFOS) is a class of specialty chemicals used in a variety of products, such as oil and water repellents, lubricants, paints, and fire-fighting foams [1]. Recently, PFOS was reported to be ubiquitously detected in the environment [2–6], as well as in human serum [7,8], raising concerns regarding its health risks. The worldwide distribution of PFOS has been attributed to its resistance to degradation by ecological systems and the rise of its bioconcentration [9–11].

The amphiphilic nature of PFOS suggests that its effects could be primarily associated with cell membrane functions. Previously, PFOS was reported to alter the activation and inactivation of L-type calcium currents ($I_{Ca,L}$) in isolated guinea-pig ventricular myocytes [12], and the observed shifts in the activation and inactivation curves were considered to arise through transmembrane potential alterations induced by PFOS condensation on the outer layer of the cell membrane. Therefore, the effects of PFOS are unlikely to be limited to myocytes or $I_{Ca,L}$. PFOS was also reported to affect the swimming behavior of a protozoan, *Paramecium caudatum*, which is regulated by voltage-dependent calcium channels [13].

Although PFOS was primarily concentrated in the liver and blood, substantially higher concentrations of PFOS were detected in the neonatal rat brain [14]. The effects of PFOS on calcium currents have raised concerns that it may have toxicological effects on the central nervous system. Here, we investigated the effects of PFOS on action potentials and currents in cultured rat cerebellar Purkinje cells using a whole-cell patch-clamp recording technique. The PFOS effects on currents through

* Corresponding author. Fax: +81 75 753 4458.
E-mail address: koizumi@pbh.med.kyoto-u.ac.jp (A. Koizumi).

0006-291X/$ - see front matter © 2006 Elsevier Inc. All rights reserved.
doi:10.1016/j.bbrc.2006.10.038

hyperpolarization-activated cyclic nucleotide-gated channels HCN1 were also studied using a *Xenopus* oocyte expression system.

Materials and methods

Drugs. Heptadecafluorooctane sulfonic acid potassium salt (purity, >98%; Fluka, Milwaukee, WI) was used as a standard for PFOS and dissolved in dimethyl sulfoxide as a 10 mM stock solution.

Primary culture of cerebellar Purkinje cells. Purkinje cells were cultured as reported previously [15,16,24]. Briefly, cerebella were dissected from Wistar rat fetuses at approximately embryonic day 20, and digested with 1% trypsin (Invitrogen, Carlsbad, CA) and 0.05% DNase (Sigma, St. Louis, MO) dissolved in 137 mM NaCl, 5 mM KCl, 7 mM Na_2PO_4, and 25 mM Hepes (pH 7.2) at 20 °C for 4 min. After washing with Ca–Mg-free Hanks' balanced salt solution (Invitrogen), the tissue was dissociated by trituration with a fire-polished Pasteur pipette in Ca-free Hanks' balanced salt solution containing 0.05% DNase and 12 mM $MgSO_4$. After centrifugation, the cell pellet was resuspended in a defined medium [15,17]. This cell suspension was plated on Petri dishes containing several heat-sterilized coverslips coated with 0.01% poly-*d*-lysine (Sigma) and cultured at 37 °C under 5% CO_2. Purkinje cells showed action potentials and robust synaptic responses during culture for at least 9 weeks.

Molecular biology. HCN1 was originally cloned from mouse brain [18]. To facilitate subcloning, 289 amino acid residues were deleted from the C-terminal region of HCN1. This C-terminal deletion had no effects on its gating kinetics or voltage-dependency, as described previously [18]. A T7 promoter sequence was introduced into the oocyte expression vector pBF [19]. HCN1 cloned into pBF was linearized by an appropriate restriction endonuclease and *in vitro*-transcribed with T7 RNA polymerase (Ambion, Austin, TX) in the presence of 2.5 mM m7G(5′)ppp(5′)G (Ambion).

Oocyte expression and electrophysiological recording. After treatment of a *Xenopus* ovary segment with 2% collagenase (Worthington, Lakewood, NJ), mature stage V and VI oocytes were manually defolliculated and isolated. Capped RNA was dissolved in sterile water at 1 mg/ml, and a 50 nl aliquot of the solution was microinjected into each oocyte using a microinjector (Nanoject; Drummond, Broomall, PA). The injected oocytes were incubated in modified Barth's medium (88 mM NaCl, 1 mM KCl, 2.4 mM $NaHCO_3$, 0.3 mM $CaNO_3$, 0.41 mM $CaCl_2$, and 0.82 mM $MgSO_4$) supplemented with 0.1 mg/ml gentamicin at 18 °C, and examined at 2–3 days after the injection using a two-electrode voltage-clamp (Axoclamp2B; Axon Instruments, Foster City, CA). The electrodes were filled with 3 M KCl and the resistance was 0.3–1.5 MΩ. Recordings were made at 25.0 ± 0.5 °C in medium containing 96 mM KCl, 1.8 mM $CaCl_2$, $MgCl_2$, 6 mM KOH, and 10 mM Hepes (buffered to pH 7.6).

Electrophysiological recordings from Purkinje cells. Cultured Purkinje cells were current- or voltage-clamped by the whole-cell patch-clamp method (EPC-8; Heka, Lambrecht, Germany) under Nomarski optics (BX50WI; Olympus, Tokyo, Japan). The compositions of the internal pipette solutions were as follows: a potassium gluconate-based pipette solution (20 mM KCl, 120 mM potassium gluconate, 0.5 mM EGTA, 10 mM Hepes (buffered to pH 7.2 with KOH)) for current-clamp and K^+ current measurements; and a cesium chloride-based pipette solution (120 mM CsCl, 0.5 mM EGTA, 10 mM Hepes (buffered to pH 7.2 with CsOH)) for Ca^{2+} or Na^+ current measurements. The composition of the external solution was as follows: 155 mM NaCl, 2.5 mM $CaCl_2$, 1 mM $MgCl_2$, 17 mM glucose, 10 mM Hepes, and 5 mM KOH (buffered to pH 7.4 with KOH) for cultured Purkinje cells. The patch pipettes were fabricated from thin-walled borosilicate glass capillaries (GS150TF-100; Harvard Apparatus, Holliston, MA) and had resistances of 3–4 MΩ. All experiments were performed at 34.0 ± 0.5 °C.

Data analysis. Data acquisition from Purkinje cells was carried out using in-house software developed on MatLab. Data acquisition for oocytes was performed using Digidata 1320 A and AxoGraph 4.8 (Axon Instruments). In both types of experiments, the currents were sampled at 10 kHz and filtered at 2 kHz. The normalized current amplitudes were plotted versus the test potentials to obtain voltage-dependent activation and inactivation curves, and fitted with a Boltzmann function. Data are presented as means ± SEM (number of experiments). Statistical differences were determined using two-tailed Student's unpaired *t*-tests, and *p* values of <0.05 were considered significant.

Results

Effects of PFOS on action potentials in cerebellar Purkinje cells

Fig. 1A shows a typical membrane potential recording from cerebellar Purkinje cells before and during exposure to PFOS. PFOS decreased the firing frequency evoked by current injection (Fig. 1B1), and the maximum rates of rise and fall were decreased (Fig. 1A, top). Fig. 1B illustrates the number of spikes during 200 ms of current injection. The number of spikes increased with increases in the injected current, although the rate of increase was smaller and the current required to generate spikes was larger after PFOS application. The resting membrane potential became slightly negative after PFOS treatment in a dose-dependent manner (Fig. 1C). The maximum rate of rise of the first spike was decreased by 10 μM PFOS (Fig. 1D), but the effect did not reach statistical significance. The same concentration of PFOS had a significantly effect on the maximum rate of fall (Fig. 1D, open columns). The level of afterhyperpolarization was slightly decreased (Fig. 1B2). Although the action potential threshold potential was decreased by 30 μM PFOS (Fig. 1E), no spontaneous firing occurred. These observations may indicate that PFOS inhibits the activity of Purkinje cells.

Since a previous study demonstrated that PFOS affected $I_{Ca,L}$ in ventricular myocytes [12], the firing pattern was further investigated after cadmium administration (500 μM). Cadmium did not affect the resting potential or firing rate (Suppl. Fig. 1A, B1, and C), but did significantly decrease the level of afterhyperpolarization and maximum rate of fall (Suppl. Fig. 1A, B2, and D). PFOS treatment with cadmium had significant effects on the resting potential (Suppl. Fig. 1B1), firing frequency (Suppl. Fig. 1C), and maximum rate of fall of the first spike (Suppl. Fig. 1D). These effects of PFOS were the same as those observed without cadmium application (Fig. 1).

Effects of PFOS on calcium, potassium, and sodium currents in cerebellar Purkinje cells

Next, we investigated the effects of PFOS on ionic currents. The calcium current was isolated by applying 1 μM tetrodotoxin (TTX) in the external solution and using a Cs^+-rich pipette solution. The effects of PFOS on steady-state inactivation were measured using a double-pulse protocol (see the pulse protocol diagram in Fig. 2A). The extent of inactivation was evaluated by the peak amplitude of the calcium current during the +20 mV test pulse (Fig. 2B). After normalization to the maximum current, the relative current amplitude was plotted against the

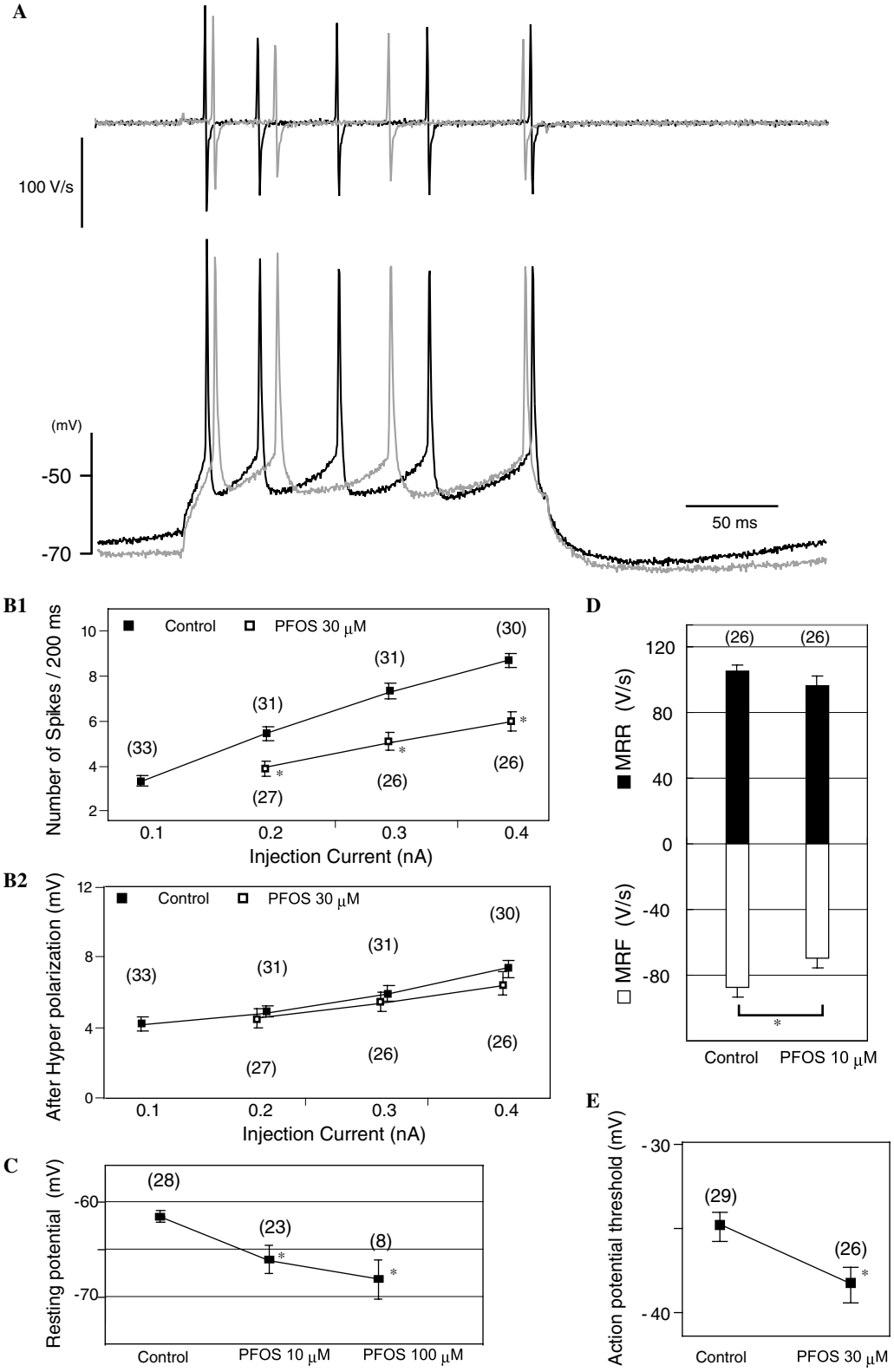

Fig. 1. Effects of PFOS on the action potential firing evoked by current injections. (A) Responses to a depolarizing current step (0.2 nA). Typical traces are shown for a control experiment (black line) and 30 μM PFOS treatment (gray line). The time derivatives of the voltage are indicated above the action potential traces. (B) Firing frequencies versus injection currents for a control experiment (filled symbols) and 30 μM PFOS treatment (open symbols). Afterhyperpolarization represents the difference between the most negative voltage reached after the current injection and the resting potential. (C) Resting potentials. (D) Maximum rates of rise (MRR; filled bars) and fall (MRF; open bars) measured for the first action potential following a current injection (0.3 nA). (E) The action potential threshold was defined as the voltage at which dV/dt exceeded 20 V/s (measured for the first action potential after a 0.3 nA current injection). Data are expressed as means ± SEM with the number of samples in parentheses. $^{*}p < 0.05$, vs. the control.

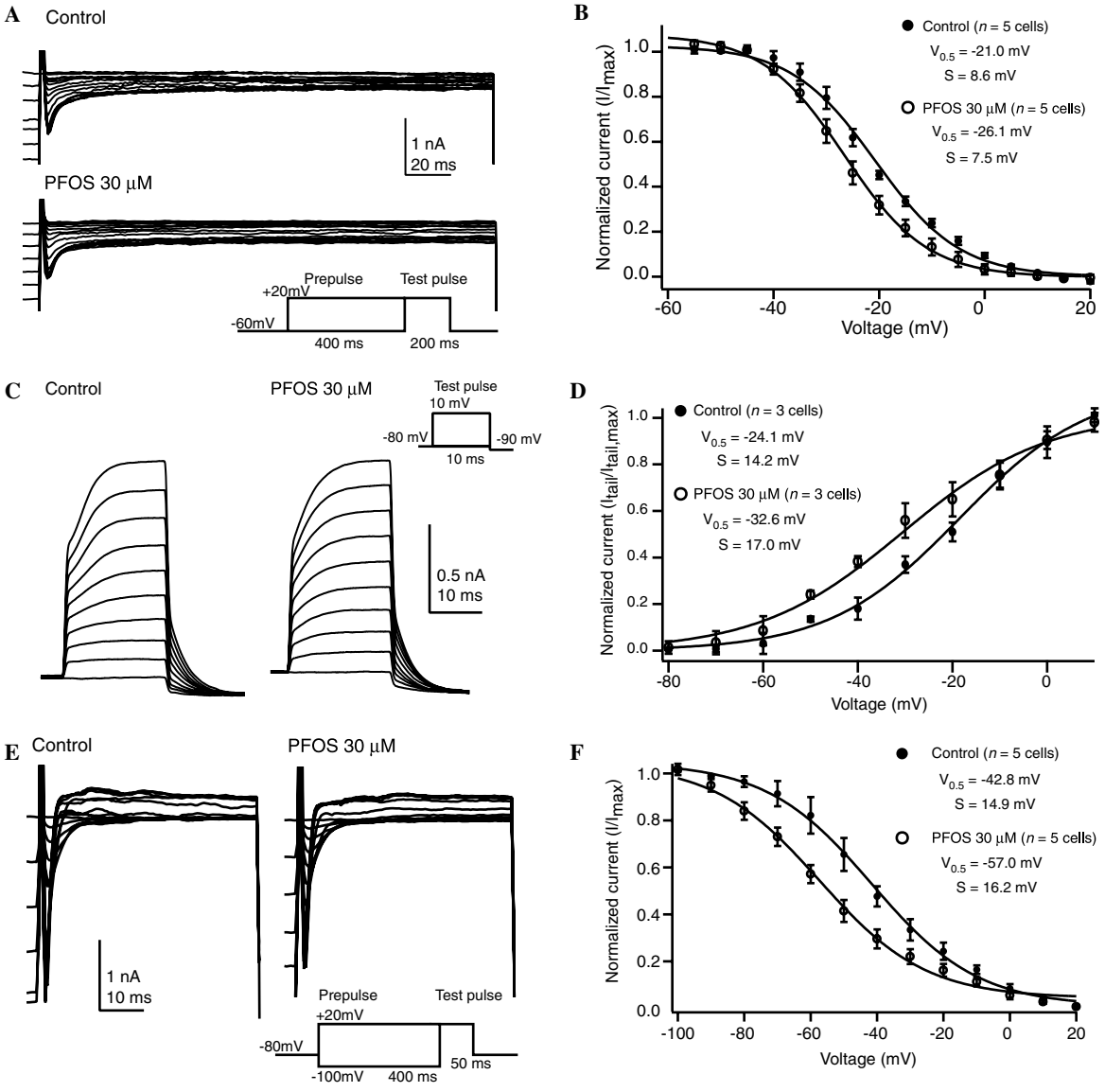

Fig. 2. Effects of PFOS on voltage-dependent inactivation and activation of Ca^{2+}, K^+, and Na^+ currents in Purkinje cells. (A) Ca^{2+} currents. Inactivation recordings showing superimposed traces of currents elicited by a depolarizing test pulse to +20 mV (200 ms), following a 400 ms prepulse between −60 and +20 mV at 5 mV increments. The voltage protocol is shown below the trace. Top: currents under the control conditions; bottom: currents after exposure to 30 μM PFOS. (B) Voltage-dependent inactivation curves. The normalized currents were plotted versus the prepulse voltage and fitted with a Boltzmann distribution. (C) K^+ currents. Tail currents obtained by stepping back to −90 mV after steps to voltages ranging from −80 to +10 mV (10 ms), starting from a V_h of −80 mV. The pulse protocol is shown on the upper right. Left: currents under the control conditions; right: currents after exposure to 30 μM PFOS. (D) Normalized tail current–voltage relationship obtained from three cells. Tail currents were measured at 2 ms after the step pulse. The normalized currents were plotted versus the test pulse voltage and fitted with a Boltzmann distribution. (E) Na^+ currents. Inactivation recordings showing superimposed traces of currents elicited by a depolarizing test pulse to +20 mV (50 ms), following a 400 ms prepulse between −100 and +20 mV in 10 mV increments. The voltage protocol is shown below the trace. Top: currents under the control conditions; right: currents after exposure to 30 μM PFOS. (F) Voltage-dependent inactivation curves. The normalized currents were plotted versus the prepulse voltage and fitted with a Boltzmann distribution.

prepulse potential (Fig. 2B). The following Boltzmann function was fitted: $I = 1/(1 + \exp((V_m - V_{0.5})/S))$, where V_m is the test potential, $V_{0.5}$ is the membrane potential for half-maximal inactivation, and S is the slope factor. $V_{0.5}$ was -21.0 ± 1.0 mV ($n = 5$ cells) for the control and -26.1 ± 1.4 mV ($n = 5$ cells) for 30 μM PFOS (t-test: $p = 0.022$), while S was 8.6 ± 1.4 mV ($n = 5$ cells) for the control and 7.5 ± 1.0 mV ($n = 5$ cells) for 30 μM PFOS (t-test: $p = 0.16$). PFOS shifted the calcium current inactivation curve toward the negative direction by 5 mV, without any significant effects on the slope factor, i.e., on the gating charge.

We next investigated the effects of PFOS on the potassium current using an external solution containing 1 μM TTX and 500 μM Cd^{2+}. The effects of PFOS on the activation were measured from tail currents using the pulse protocol indicated in Fig. 2C. PFOS did not appear to affect the potassium current. The amplitude of the tail

current reflects the conductance immediately before the step changes to −90 mV. The amplitude of the potassium tail current measured at 2 ms after the step changes was not affected by PFOS (0.50 nA for the control vs. 0.53 nA for PFOS after activation at +10 mV). These tail current amplitudes were normalized to the maximum tail current and plotted against the membrane potential that activated the current (Fig. 2D). The curve was fitted with the Boltzmann function and $V_{0.5}$ was -24.1 ± 1.2 mV ($n = 3$ cells) for the control and -32.6 ± 2.7 mV ($n = 3$ cells) for 30 μM PFOS (t-test: $p = 0.045$), and S was 14.2 ± 2.3 mV ($n = 3$ cells) for the control and 17.0 ± 3.1 mV ($n = 3$ cells) for 30 μM PFOS (t-test: $p = 0.5$). These results indicate that PFOS shifted the activation curve of potassium conductance toward the negative direction by 8 mV, while the gating charge remained unaffected.

The effects of PFOS on the sodium current were investigated using a 500 μM Cd^{2+}-containing external solution and a Cs^{+}-rich pipette solution. The effects of PFOS on the steady-state inactivation were measured using a double-pulse protocol (see the pulse protocol in Fig. 2E). The extent of inactivation was evaluated by plotting the normalized amplitude of the sodium current to the prepulse potential (Fig. 2F), and then fitted with the Boltzmann function, and $V_{0.5}$ was -42.8 ± 4.1 mV ($n = 5$ cells) for the control and -57.0 ± 2.6 mV ($n = 5$ cells) for 30 μM PFOS (t-test: $p = 0.020$), and S was 14.9 ± 2.1 mV ($n = 5$ cells) for the control and 16.2 ± 1.5 mV ($n = 5$ cells) for 30 μM PFOS (t-test: $p = 0.6$). These results indicate that PFOS shifted the sodium channel inactivation curve toward the negative direction by 15 mV, while the gating charge remained unaffected.

Effects of PFOS on the HCN1 current expressed in oocytes

HCN1 was transiently expressed in *Xenopus* oocytes and examined using the 2-electrode whole-cell voltage-clamp technique, with a holding potential of −20 mV. The tail-current amplitudes were measured at 2–3 ms after a step pulse to −120 mV. HCN1 showed robust inward currents by hyperpolarizing voltage steps (Suppl. Fig. 2A). The normalized tail current amplitudes were plotted against the test potentials to obtain the voltage-dependent activation curve and fitted with the Boltzmann function (Suppl. Fig. 2B), and $V_{0.5}$ was -87.6 ± 1.5 mV ($n = 5$ cells) for the control and -120.7 ± 2.5 mV ($n = 5$ cells) for 30 μM PFOS (t-test: $p < 0.001$), and S was 15.0 ± 1.9 mV ($n = 5$ cells) for the control and 18.1 ± 2.5 mV ($n = 5$ cells) for 30 μM PFOS (t-test: $p = 0.06$). The voltage-dependence of the HCN1 channel activation was affected by PFOS, since PFOS shifted the activation curve toward the negative direction by 33 mV, although the gating charge was unaffected.

Taken together, these observations demonstrate that PFOS affects the gating properties of various ionic channels, and that the effects involved negative shifts of the voltage-dependence. These findings may be related to the membrane affinity of PFOS and its negative charge.

Discussion

PFOS altered the activation and inactivation of I_{Ca}, I_{Na}, I_K, and I_{HCN1} toward the hyperpolarized direction. These findings are comparable with a previous report on the effects of PFOS on $I_{Ca,L}$ in isolated guinea-pig ventricular myocytes [12]. The effects of PFOS on the properties of the ionic currents appeared to be consistent among different current types and cells. Therefore, we consider that the shifts in the activation and inactivation curves are due to changes in the surface potential of the cell membrane. It is well known in excitable membranes that an increase in the external Ca^{2+} ion concentration produces a positive shift of the critical membrane potential [20–22]. This phenomenon was previously explained on the basis of a diffuse double layer generated on the fixed negative charges at the surface of the membrane [23]. It was proposed that Ca^{2+} ions are adsorbed on the surface of the membrane and alter the surface potential toward the positive direction, thereby making the effective electrical field within the membrane steeper and producing depolarizing shifts of the gating kinetics of ionic channels [20]. Incorporation of PFOS into the outer cell membrane may affect the gating properties of ionic channels in the reverse direction by increasing the negative surface charge density, thereby rendering the transmembrane potential gradient less steep and resulting in hyperpolarizing shifts of both the activation and inactivation of voltage-gated ionic channels.

Activation of I_{HCN1} expressed in *Xenopus* oocytes produced a more negative shift of 37 mV compared to the currents observed in Purkinje cells. If PFOS affects the voltage-dependence of ionic currents through alterations in the surface membrane potential, the effects would depend on the external environment of the membrane, including the external ionic strength, as well as the surface distribution of phospholipids and their composition in different cells and expression systems.

PFOS reduced the firing rate and hyperpolarized the resting membrane potential. These effects were also observed in the presence of cadmium suggesting that PFOS not only modulated I_{Ca} but had effects on a variety of ionic currents. In particular, the hyperpolarizing shift of I_K activation may lead to decreases in the input resistance and firing frequency. The hyperpolarizing shift of the gating properties of I_{HCN1} may increase the input impedance of a cell, although the extent is dependent on the expression level of the HCN1 channels.

In conclusion, PFOS demonstrated general inhibitory effects on action potentials in cultured cerebellar Purkinje cells in the present study. However, the possible toxic effects of PFOS on the central nervous system in vivo remain to be investigated.

Acknowledgments

This study was supported by Grants-in-Aid from the Ministry of Education, Culture, Sports, Science and

Technology (17023027-0133), the Ministry of Health, Labour and Welfare (H15-Chemistry-004), the Japan Society for the Promotion of Science (17-1910), and the Showa Shell Sekiyu Foundation (2005-A038).

Appendix A. Supplementary data

Supplementary data associated with this article can be found, in the online version, at doi:10.1016/j.bbrc.2006.10.038.

References

[1] OECD, Hazard assessment of perfluorooctane sulfonate and its salts, 2002. Available from: <http://www.oecd.org/dataoecd/23/18/2382880.pdf>.
[2] B. Boulanger, A.M. Peck, J.L. Schnoor, K.C. Hornbuckle, Mass budget of perfluorooctane surfactants in Lake Ontario, Environ. Sci. Technol. 39 (2005) 74–79.
[3] N. Saito, K. Harada, K. Inoue, K. Sasaki, T. Yoshinaga, A. Koizumi, Perfluorooctanoate and perfluorooctane sulfonate concentrations in surface water in Japan, J. Occup. Health 46 (2004) 49–59.
[4] K. Harada, S. Nakanishi, K. Sasaki, K. Furuyama, S. Nakayama, N. Saito, K. Yamakawa, A. Koizumi, Particle size distribution and respiratory deposition estimates of airborne perfluorooctanoate and perfluorooctanesulfonate in Kyoto area, Japan, Bull. Environ. Contam. Toxicol. 76 (2006) 306–310.
[5] K. Kannan, J.W. Choi, N. Iseki, K. Senthilkumar, D.H. Kim, S. Masunaga, J.P. Giesy, Concentrations of perfluorinated acids in livers of birds from Japan and Korea, Chemosphere 49 (2002) 225–231.
[6] S. Nakayama, K. Harada, K. Inoue, K. Sasaki, B. Seery, N. Saito, A. Koizumi, Distributions of perfluorooctanoic acid (PFOA) and perfluorooctane sulfonate (PFOS) in Japan and their toxicities, Environ. Sci. 12 (2005) 293–313.
[7] A.M. Calafat, L.L. Needham, Z. Kuklenyik, J.A. Reidy, J.S. Tully, M. Aguilar-Villalobos, L.P. Naeher, Perfluorinated chemicals in selected residents of the American continent, Chemosphere 63 (2006) 490–496.
[8] K. Harada, N. Saito, K. Inoue, T. Yoshinaga, T. Watanabe, S. Sasaki, S. Kamiyama, A. Koizumi, The influence of time, sex and geographic factors on levels of perfluorooctane sulfonate and perfluorooctanoate in human serum over the last 25 years, J. Occup. Health 46 (2004) 141–147.
[9] K. Kannan, L. Tao, E. Sinclair, S.D. Pastva, D.J. Jude, J.P. Giesy, Perfluorinated compounds in aquatic organisms at various trophic levels in a great lakes food chain, Arch. Environ. Contam. Toxicol. 48 (2005) 559–566.
[10] A. Morikawa, N. Kamei, K. Harada, K. Inoue, T. Yoshinaga, N. Saito, A. Koizumi, The bioconcentration factor of perfluorooctane sulfonate is significantly larger than that of perfluorooctanoate in wild turtles (*Trachemys scripta elegans* and *Chinemys reevesii*): an Ai river ecological study in Japan, Ecotoxicol. Environ. Saf. 65 (2006) 14–21.
[11] K. Harada, K. Inoue, A. Morikawa, T. Yoshinaga, N. Saito, A. Koizumi, Renal clearance of perfluorooctane sulfonate and perfluorooctanoate in humans and their species-specific excretion, Environ. Res. 99 (2005) 253–261.
[12] K. Harada, F. Xu, K. Ono, T. Iijima, A. Koizumi, Effects of PFOS and PFOA on L-type Ca^{2+} currents in guinea-pig ventricular myocytes, Biochem. Biophys. Res. Commun. 329 (2005) 487–494.
[13] E. Matsubara, K. Harada, K. Inoue, A. Koizumi, Effects of perfluorinated amphiphiles on backward swimming in *Paramecium caudatum*, Biochem. Biophys. Res. Commun. 339 (2006) 554–561.
[14] C. Lau, J.R. Thibodeaux, K. Das, D.J. Ehresman, S. Tanaka, J. Froehlich, J.L. Butenhoff, evaluation of perfluorooctane sulfonate in the rat brain, Toxicologist 90 (2006) S118. Abstract ID: 576.
[15] A. Weber, M. Schachner, Maintenance of immunocytologically identified Purkinje cells from mouse cerebellum in monolayer culture, Brain Res. 311 (1984) 119–130.
[16] T. Hirano, H. Ohmori, Voltage-gated and synaptic currents in rat Purkinje cells in dissociated cell cultures, Proc. Natl. Acad. Sci. USA 83 (1986) 1945–1949.
[17] G. Fischer, Cultivation of mouse cerebellar cells in serum free hormonally defined media: survival of neurons, Neurosci. Lett. 28 (1982) 325–329.
[18] T.M. Ishii, M. Takano, H. Ohmori, Determinants of activation kinetics in mammalian hyperpolarization-activated cation channels, J. Physiol. 537 (2001) 93–100.
[19] B. Fakler, S. Herlitze, B. Amthor, H.P. Zenner, J.P. Ruppersberg, Short antisense oligonucleotide-mediated inhibition is strongly dependent on oligo length and concentration but almost independent of location of the target sequence, J. Biol. Chem. 269 (1994) 16187–16194.
[20] B. Frankenhaeuser, A.L. Hodgkin, The action of calcium on the electrical properties of squid axons, J. Physiol. 137 (1957) 218–244.
[21] D.E. Goldmann, A molecular structural basis for the excitation properties of axons, Biophys. J. 4 (1964) 167–188.
[22] B. Hille, Charges and potentials at the nerve surface. Divalent ions and pH, J. Gen. Physiol. 51 (1968) 221–236.
[23] H. Ohmori, M. Yoshii, Surface potential reflected in both gating and permeation mechanisms of sodium and calcium channels of the tunicate egg cell membrane, J. Physiol. 267 (1977) 429–463.
[24] K. Takatsuka, T.M. Ishii, H. Ohmori, A novel Ca^{2+} indicator protein using FRET and calpain-sensitive linker, Biochem. Biophys. Res. Commun. 336 (2005) 316–323.